Spontaneous firing statistics and information transfer in electroreceptors of paddlefish

Article *in* Physical Review E · December 2008

DOI: 10.1103/PhysRevE.78.051922 · Source: PubMed

2 authors:

I.A. Fuwape
Federal University of Technology, Akure
39 PUBLICATIONS **156** CITATIONS
SEE PROFILE

Alexander B Neiman
Ohio University
176 PUBLICATIONS **4,669** CITATIONS
SEE PROFILE

Spontaneous firing statistics and information transfer in electroreceptors of paddlefish

Ibiyinka Fuwape*
Department of Physics and Astronomy, Ohio University, Athens, Ohio 45701, USA

Alexander B. Neiman†
Department of Physics and Astronomy and Quantitative Biology Institute, Athens, Ohio 45701, USA

(Received 25 September 2008; published 24 November 2008)

We study information processing in a peripheral sensory receptor system which possesses spontaneous dynamics with two distinct rhythms. Such organization was found in the electrosensory system of paddlefish and is represented by two distinct and unidirectionally coupled oscillators, resulting in biperiodic spontaneous firing patterns of sensory neurons. We use computational modeling to elucidate the functional role of spontaneous oscillations in conveying information from sensory periphery to the brain. We show that biperiodic organization resulting in nonrenewal statistics of background neuronal activity leads to significant improvement in information transfer through the system as compared to an equivalent renewal model.

DOI: 10.1103/PhysRevE.78.051922 PACS number(s): 87.19.ln, 87.19.lo, 05.40.−a

I. INTRODUCTION

Rhythmic spontaneous activity was observed in various peripheral sensory systems. Endogenous rhythms were found in auditory and vestibular peripheral systems in the form of mechanical oscillations of hair bundles of sensory cells [1–3], receptor potential oscillations [4,5], and pacemaker-type firing of sensory vestibular afferent neurons [6]. These sensory receptors have a specific structure where detector hair cells in a sensory epithelium excite primary afferent neurons. Recent studies have shown that spontaneous mechanical oscillations of hair bundles in auditory hair cells of lower vertebrates are responsible for extreme sensitivity and selectivity of auditory system [7]. However, functional role of spontaneous oscillations of hair cells' membrane potential observed in Ref. [4] is unclear. Ampullary electroreceptors, those that are found in several aquatic animals, have structure similar to auditory and vestibular receptors mentioned above. Hair cell-type receptor cells are coupled via excitatory synapses to sensory afferent neurons which send their axons to the brain. Spontaneous noisy transepithelial 20–30 Hz oscillations were reported in electroreceptors of skates [8–10]. The functional role of these oscillations was hypothesized to be in secretion of neurotransmitter which is necessary to account for observed background periodic firing of sensory afferent neurons [10]. Two distinct types of oscillators were found in peripheral ampullary electroreceptors of paddlefish. The first type resides in population of epithelial cells, while the second type resides in the terminals of sensory afferent neurons [11,12]. Similarly to skate electroreceptors the fundamental frequency of epithelial oscillations is at 26 Hz (at room temperature) and is not affected by external electric field stimuli [12]. Unidirectional coupling of epithelial oscillator to afferent oscillator, oscillating with fundamental frequency in the range 30–70 Hz, results in quasi-periodic dynamics of the system (see Fig. 1 in Refs. [12,30] for a cartoon showing the organization of the paddlefish electroreceptors). The frequency content of natural stimuli which may be encountered by paddlefish is in the range 0.5–20 Hz [13–16] and the frequency response of electroreceptors matches this range [16,17]. Thus, a possible role of epithelial oscillations in electroreceptors must be different from that in auditory receptors, whereby self-sustained oscillations of hair cell bundles are synchronized by weak external stimuli leading to strong and sharp resonances. Rather, since the frequency of these oscillations is invariant with respect to external stimuli, the epithelial oscillations may be considered as source of narrow-band internal noise which makes a major contribution to the variability of spontaneous receptor's dynamics [11,12].

A distinctive property of spontaneous dynamics of paddlefish electroreceptors is nonrenewal statistics of their firing patterns [11,12], which is evident from extended serial correlation of afferents' interspike intervals (ISI). Nonrenewal statistics of spontaneous neuronal firing was a subject of several recent studies [18–22]. In particular, several studies have elucidated the role of negative serial correlations of sensory neurons of *P*-type electroreceptors in improving information transfer [18,19,23]. The effect of enhancement of information transfer was explained in terms of shaping the power spectrum of background activity [23,24]. Nonrenewal stochastic dynamics observed in these studies resulted from internal properties of neurons, such as spike-frequency adaptation [25–27] or threshold fatigue [19,28,29]. In contrast, we have shown that extended serial correlations in paddlefish electroreceptors are mainly due to epithelial oscillations exciting afferent neurons [12,30]. Furthermore, the structure of serial correlations and their correlation length is determined by the frequency ratio of epithelial to afferent oscillators frequencies. These serial correlations leads to significant reduction of noise power in low frequency band and thus may lead potentially to enhancement of encoding of low-frequency stimuli [30]. In this work we use a simple computational model [30] based on so-called theta neuron model [31–33] to study the significance of the receptor oscillations in encoding of weak external time-varying stimuli by sensory receptors.

*Also at: Department of Physics, Federal University of Technology, Akure, PMB 704, Nigeria.
†neimana@ohio.edu

The parameters of the model were tuned to reproduce statistical properties of spontaneous dynamics of electroreceptors in paddlefish. To elucidate the role of nonrenewal dynamics induced by receptor's oscillations we compared information transmission through the original model with oscillations to a renewal model which possesses the same first-order statistics but lacks epithelial oscillations and thus serial ISI correlations.

II. MODEL AND METHODS

A. Model

We model stochastic biperiodic dynamics of electroreceptors as unidirectional coupling of epithelial oscillators, represented by a stochastic narrow-band process, to a self-sustained oscillating neuron, which we model using so-called theta neuron model. Theta neuron model is a canonical model for type-I spiking [31,33] and is equivalent to an integrate and fire neuron with quadratic nonlinearity. It was successfully employed to study various aspects of neuronal dynamics, including stochastic dynamics of neurons [34,35], synchronization in neuronal networks and emergence of rhythms [36,37], to name a few. A modified version of this model was used to study spontaneous dynamics of biperiodic electroreceptors in Ref. [30]. The dynamics of afferent neuron is given by the phase variable θ defined on a circle: $\dot{\theta}=1-\cos\theta+R(1+\cos\theta) \bmod 2\pi$, where R is the parameter related to external current applied to the neuron. The theta neuron "fires" when $\theta(t)$ crosses π so that the spike train produced by the model is $x(t)=\Sigma\delta[\theta(t)-\pi]$, where summation is taken over crossing events. For negative values of R the system is excitable with a pair of stable and unstable equilibria. For positive values of R the theta neuron fires periodically at the rate $\sqrt{R}/\pi$. In our case the parameter R is timedependent and is modulated by the epithelial oscillations signal $e(t)$, a broad-band noise $\xi(t)$ and by time-dependent stimulus $y(t)$. We also included a slow adaptation $u(t)$ [32] to account for short-range negative correlations observed in experiments when epithelial oscillations were absent [11]. The model equations are

$$\dot{\theta}=1-\cos\theta+(1+\cos\theta)[R_0+e(t)+\xi(t)-u+y(t)] \bmod 2\pi,$$

$$\dot{u}=-\lambda u+s\delta(\theta-\pi). \tag{1}$$

In Eq. (1) R_0 stands for the constant component of the current which sets the fundamental frequency of afferent oscillator. The second equation describes slow adaptation $u(t)$, where λ is the rate of adaptation $\lambda \ll \sqrt{R_0}/\pi$ and s is the strength of adaptation. The epithelial oscillations arising in a population of cells is modeled by zero-mean Gaussian narrow-band process $e(t)$ with the power spectrum

$$P_{ee}(f)=\frac{\Delta f_0^2 A^2}{(f^2-f_0^2)^2+\Delta^2 f^2}, \tag{2}$$

where A is the standard deviation of the process, f_0 is the natural frequency, and Δ determines the width of the spectral line $\Delta \ll f_0$. In simulations $e(t)$ was obtained by solving linear stochastic differential equations for a linear damped oscillator perturbed by Gaussian white noise [38]. The broadband noise $\xi(t)$ in Eq. (1) was modeled by exponentially correlated Ornstein-Uhlenbeck process with the intensity D and correlation time τ_c. The autocorrelation function of this process is given by [39]

$$\langle \xi(t)\xi(t+\tau)\rangle=\frac{D}{\tau_c}\exp\left(-\frac{|\tau|}{\tau_c}\right). \tag{3}$$

The correlation time τ_c was chosen to be much smaller than any other time scale in the system, so that noise $\xi(t)$ is effectively white.

The model equations (1)–(3) are dimensionless, resulting in a sequence of spike times t_n, when θ crosses π. We used experimental data from paddlefish electroreceptors to choose parameter values for the dimensionless model. Epithelial oscillations (EOs) result from the collective activity of hundreds of cells in the epithelial layer of electroreceptors. The fundamental frequency of the EO in different electroreceptors and in different paddlefish is very similar 26 ± 1.6 Hz, at room temperature (22 °C) with the width of the spectral peak 1.7 ± 0.4 Hz [12]. In contrast to the EO, the fundamental frequency of the afferent oscillator (AO) is distributed over a wide range of 30–70 Hz for different afferents in different fish [12]. The ratio of epithelial to afferent oscillator frequencies is $w=0.49\pm0.08$. As in Ref. [30] we use the period of the EO as a reference time scale for the model. In the following we fix dimensionless frequency of the EO in Eq. (2) at $f_0=1/2\pi$. Then the parameter R_0 is chosen such that the ratio of epithelial to afferent oscillators frequencies w is around 0.5, as in experimental data. Other dimensionless parameters determining time scales were chosen as $\lambda=0.02$, $\Delta=0.05f_0$, $\tau_c=0.02$. The transition from dimensionless time to time in seconds is given by $t(\mathrm{s})=t/(2\pi f_e)$, where $f_e=26$ Hz is the EO frequency. In practice, we integrated numerically dimensionless model equations and then renormalized dimensionless spike times to spike times in seconds for further processing [30]. In the following we always keep the frequency of the EO f_e constant while changing the parameter R_0 which leads to the change of the frequency of the AO, f_a and thus to the change of the frequency ratio $w=f_e/f_a$. Time varying stimulus $y(t)$ in Eq. (1) is Gaussian band-limited noise with cutoff frequency f_c and standard deviation σ, which was obtained by linear filtering of white noise as in Ref. [29]. Stimulus variance was kept constant while varying cutoff frequency, so that the power spectrum of the stimulus is given by $P_{yy}=2\sigma^2/f_c$.

B. Measures of variability and response

The spike train generated by the model was constructed as a sum of delta functions centered at spike times t_n:

$$x(t)=\Sigma_n\delta(t-t_n) \tag{4}$$

with ISI $T_n=t_n-t_{n-1}$, $n=1,\ldots,N$, where N is the total number of spikes in a train. The mean firing rate $\langle f\rangle$ was calculated as reciprocal to the mean interspike interval $\langle f\rangle=1/\langle T_n\rangle$.

Several measures were used to characterize variability of spontaneous dynamics when the stimulus was turned off, $\sigma=0$. First order statistics included the probability density of ISI and the coefficient of variation of ISI calculated as the ratio of standard deviation of ISI to the mean ISI: cv $=\mathrm{std}(T_n)/\langle T_n\rangle$. The second order statistics measures included normalized autocorrelation function of ISI, also known as the serial correlation coefficient (SCC), and the power spectrum of the spike train [40]. The SCC was calculated as

$$C(k)=\frac{\langle T_nT_{n+k}\rangle-\langle T_n\rangle^2}{\langle T_n^2\rangle-\langle T_n\rangle^2}. \tag{5}$$

The extension of serial correlation was characterized by the correlation length

$$t_{\mathrm{cor}}=\sum_{k=1}^{\infty}|C(k)|. \tag{6}$$

The power spectrum of a spike train was calculated as in Ref. [40].

The response of the model to external stimulus $y(t)$ was characterized in terms of the system gain $H(f)$ and the coherence function $\Gamma(f)$ [41],

$$H(f)=\frac{|P_{xy}(f)|}{P_{yy}(f)}, \tag{7}$$

$$\Gamma(f)=\frac{|P_{xy}(f)|^2}{P_{xx}(f)P_{yy}(f)}, \tag{8}$$

where $P_{xy}(f)$ is the cross-spectral density of the spike train $x(t)$ and stimulus $y(t)$; $P_{xx}(f)$ and $P_{yy}(f)$ are power spectral densities (PSDs) of the spike train and stimulus, respectively. The coherence function is a normalized measure of cross-correlations between stimulus and neural response and ranges between 0 and 1. It can be related to the lower bound of mutual information rate by [42–44]

$$\mathcal{I}=-\int_0^{f_c}\log_2[1-\Gamma(f)]df, \tag{9}$$

in units of bits per second. In the following we normalize the information rate by the mean firing rate $\mathcal{I}/\langle f\rangle$, which gives the information rate in units of bits per spike [44].

C. Nonrenewal and renewal models

In order to elucidate the role of epithelial oscillations in information transmission through the system we compared response properties of the original model (1) to a modified model in which the EO and slow adaptation were turned off, $A=0$, $s=0$:

$$\dot{\theta}_r=1-\cos\theta_r+(1+\cos\theta_r)[R_r+\xi(t)+y(t)]. \tag{10}$$

In the absence of stimulus ($\sigma=0$) this modified model generates spike trains with statistics close to renewal and is determined by two parameters: R_r and noise intensity D_r. In the following we call this model "renewal." First-order statistics of spontaneous firing is determined by the probability density of ISI [45]. For a given parameter set of the original model (1) the parameters of the renewal model R_r and D_r were changed until the probability density of ISI of renewal model $p_r(T)$ matched the ISI probability density of the original model $p(T)$. The closeness of two ISI distributions was characterized by the Kullback-Leibler distance [46,47]

$$K[p,p_r]=\int p_r(T)\ln\frac{p_r(T)}{p(T)}dT. \tag{11}$$

Thus, for a given set of parameters of the original model the numerical procedure was as follows.

(i) Stimulus $y(t)$ was turned off, $\sigma=0$, and ISI distribution of the original model $p(T)$ was estimated. (ii) Two parameters of the renewal model were changed to minimize the Kullback-Leibler distance (11) between $p(T)$ and $p_r(T)$. This step gave parameter values of the renewal model providing the best match of the first order statistics for the original and renewal models. (iii) Stimulus $y(t)$ was applied to both models; coherence functions and information rates were calculated and compared. Numerical simulations of Eqs. (1) and (10) were conducted using the Euler scheme with the time step 10^{-3}, and the duration of simulation for each parameter value was equivalent to 10 min.

Figure 1 shows an example of application of steps (i) and (ii) described above to a particular set of parameters. Probability density of ISIs of the original model (1) is shown in Fig. 1(a) by solid (red) line, reflecting spontaneous firing with the mean firing rate of 60.7 Hz and CV=0.177. Parameters R_r and D_r of the renewal model (10) were tuned to minimize the Kullback-Leibler distance shown in Fig. 1(b). The dashed (blue) line in Fig. 1(a) shows ISIs probability density of the renewal model $p_r(T)$, calculated for the parameter values obtained by minimization of the $K[p,p_r]$. Both probability densities perfectly match. Second-order statistics of original model is characterized by extended serial correlations [Fig. 1(c)] and by the power spectral density with characteristic structure of peaks [Fig. 1(d)]. The EO and AO are represented by the peaks at f_e and f_a, respectively, along with the sidebands at $f_a\pm f_e$. As expected, the modified model (10) is characterized by renewal statistics verified by δ-correlated ISI, dashed (blue) line in Fig. 1(c). Comparison of power spectral densities of two models [Fig. 1(d)] reveals the effects of EO and extended serial correlations: (i) the power at low frequency of the original model is an order of magnitude lower than that of the renewal model; (ii) the width of afferent spectral peak at f_a is significantly narrower for the original model.

III. RESULTS

A. Coherence and gain for original and renewal models

The transfer (gain) functions, $H(f)$ of the original and renewal models are shown in Fig. 2(a). For a given parameter set, the gain functions of both models are very close except at low frequencies $f\leqslant 1$ Hz, where the gain of the original model [solid (red) line in Fig. 2(a)], increases with frequency owing to high-pass filtering effect of adaptation [27]. When adaptation was turned off [$s=0$, dotted (green)

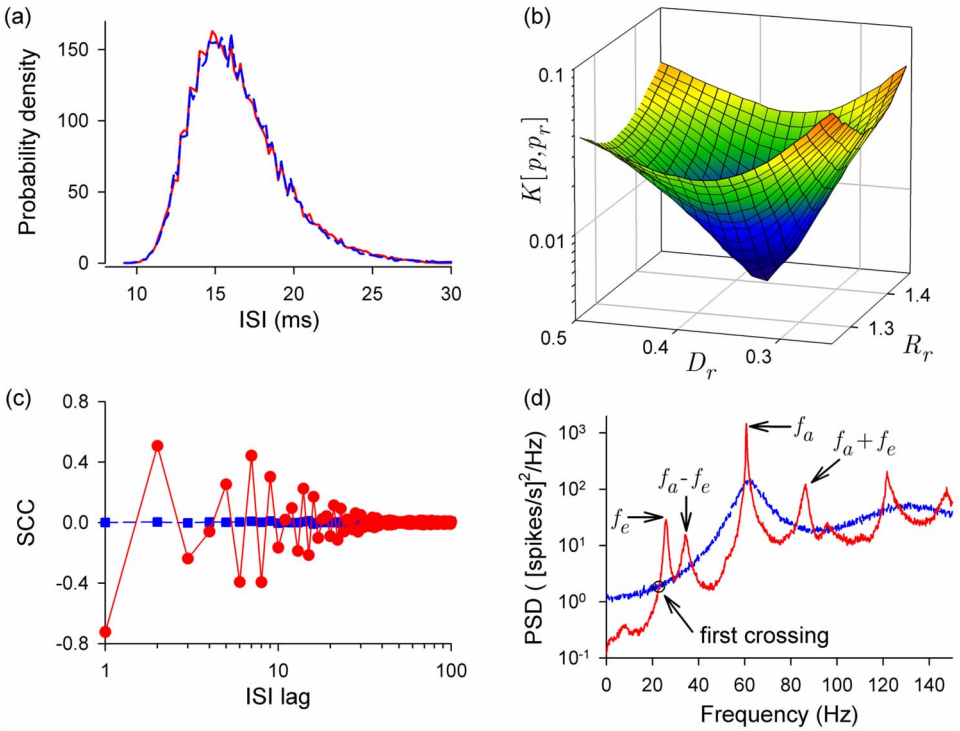

FIG. 1. (Color online). Spontaneous dynamics of the original and renewal models. Solid (red) lines and dashed (blue) lines correspond to the original and renewal models, respectively. Parameters of the original model were $R_0=7$, $A=0.5$, $D=0.02$, $s=0.3$, $\lambda=0.02$, $s=0.3$, $1/\tau_c=50$. (a) Probability densities of ISI. (b) Kullback-Leibler distance (11) as a function of the parameters of renewal model R_r and D_r. $K[p,p_r]$ possesses global minimum at $R_r=1.363$ and $D_r=0.355$. These parameter values were used for simulation of the renewal model shown by dashed (blue) lines in panels (a), (c), and (d). (c) Serial correlation coefficients (SCC) of ISIs; circles and squares correspond to the original and renewal models, respectively. (d) Power spectral densities (PSD) of spontaneous spike trains generated by the original and renewal models. f_a, afferent oscillator peak. f_e, epithelial oscillator peak. The circle indicates the first crossing of PSDs.

line in Fig. 2(a)] but epithelial oscillations were still presented the gain functions of both model were close within the whole stimulus frequency band. For this case of no adaptation the same procedure of tuning the parameters R_r and D_r was used as described in Sec. II C. In contrast, the coherence functions of the original model is significantly (2–2.5 times) larger than that of renewal model [Fig. 2(b)]. This clearly indicated that the external signal was transmitted more efficiently by the original model than by the renewal model. The mutual information rates $\mathcal{I}$ estimated from these coherence functions were 0.33 bit/spike for the original model and 0.10 bit/spike for the renewal model. Slow adaptation had a small effect on both the coherence function and on the mutual information rate. This improvement of signal transmission can be explained using the concept of noise shaping [19,23]. In the linear response approximation the coherence function can be written as [48]

$$\Gamma(f) = \frac{|H(f)|^2 P_{yy}(f)}{P_{xx}^{(0)}(f) + |H(f)|^2 P_{yy}(f)}, \tag{12}$$

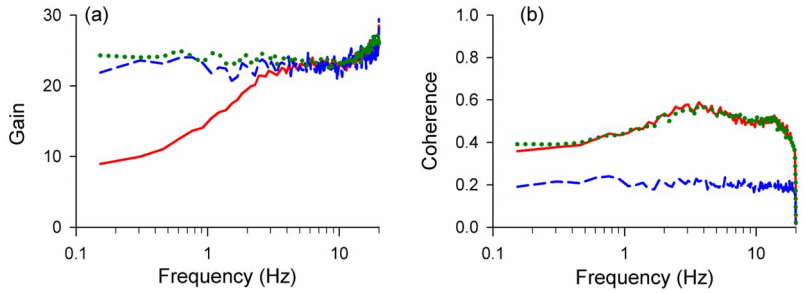

FIG. 2. (Color online). Gain (a) and coherence functions (b) for the original and renewal models stimulated with band-limited Gaussian noise with cutoff frequency $f_c=20$ Hz and standard deviation $\sigma=0.2$. In both panels dashed (blue) lines correspond to the renewal model; solid (red) lines correspond to the original model with $R_0=7$, $s=0.3$, $D=0.02$; dotted (green) lines correspond to the original model with $R_0=1.43$, $s=0$, $D=0.02$. The parameters of the renewal model were tuned to match first-order spontaneous statistics of the original model.

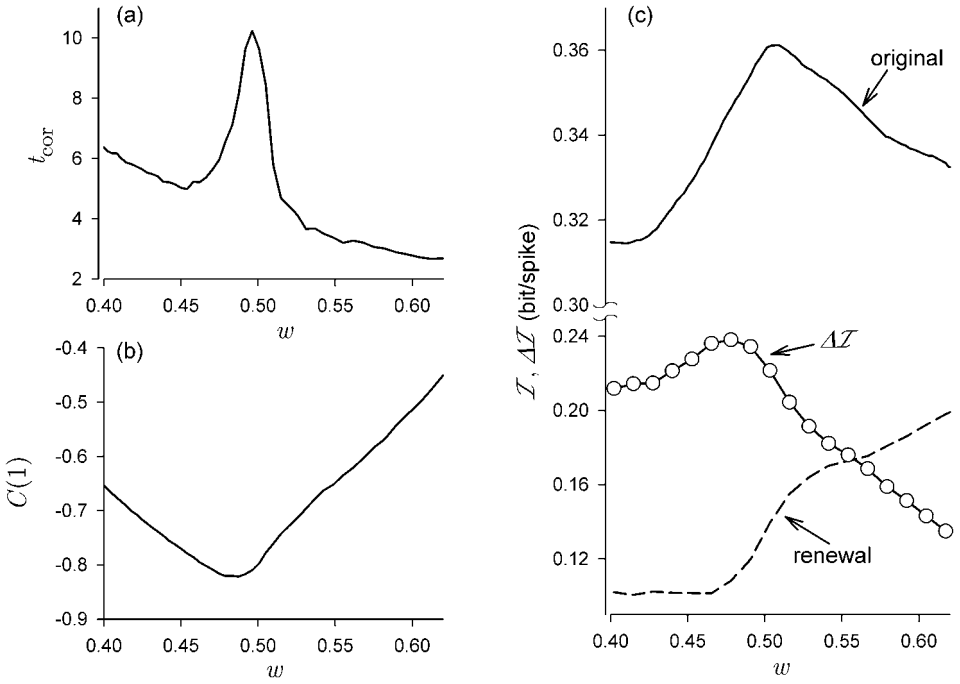

FIG. 3. Dependence of ISI correlations and information transfer on the ratio of the afferent to epithelial oscillation frequencies $w=f_e/f_a$. ISI correlation length (a) and the first lag of SCC (b) versus w for spontaneous firing of the original model. Mutual information rates for the original (solid line) and renewal (dashed line) models and the difference $\Delta\mathcal{I}=\mathcal{I}_{\text{original}}-\mathcal{I}_{\text{renewal}}$ (circles), versus w. In numerical simulations we varied the parameter R_0 of the original model (1) changing the frequency of AO f_a, while the frequency of EO f_e was fixed. The stimulus parameters were $f_c=20$ Hz, $\sigma=0.2$. Other parameters were the same as in Fig. 1.

where $P_{xx}^{(0)}(f)$ is PSD of spontaneous firing representing background noise in the system. According to Eq. (12) the smaller is $P_{xx}^{(0)}$ the larger is the coherence. PSD of spontaneous firing of the original model displays significantly less power in the stimulus frequency range as compared to renewal model [see Fig. 1(d)] hence leading to increased coherence and information rate.

B. Information rate versus frequency ratio of two oscillators

The structure of ISI serial correlations is determined by the ratio of frequencies of epithelial to afferent oscillators $w=f_e/f_a$ [30]. The longest and strongest serial ISI correlations were observed for w close to 0.5: the correlation length is maximal at $w=0.5$, while the first correlation lag of SCC is minimal at $w=0.48$. This is illustrated in Figs. 3(a) and 3(b) by showing the ISI correlation length and the first lag of the SCC versus the frequency ratio w, where the mean firing rate f_a was varied by changing R_0. The increase in ISI correlation length led to enhancement in signal transmission as shown in Fig. 3(c). Mutual information rate of the original model possessed a maximum at $w=0.5$. The difference between the information rate of the original and renewal models $\Delta\mathcal{I}=\mathcal{I}_{\text{original}}-\mathcal{I}_{\text{renewal}}$ characterizes the enhancement of signal transmission or information gain due to the presence of ISI correlations in the original model. $\Delta\mathcal{I}$ shows nonmonotonous dependence on the frequency ratio with a maximum at $w=0.48$, as indicated in Fig. 3(c).

C. Information rate versus stimulus parameters

Figure 4(a) shows the dependence of information rate versus stimulus strength for a fixed stimulus bandwidth ($f_c=20$ Hz). Mutual information rates of both models increases with the increase of stimulus strength. However, mutual information rate of the original model increases faster than that of the renewal model, resulting in significant information gain $\Delta\mathcal{I}$. Furthermore, information gain shows nonmonotonous dependence passing trough a maximum at small stimulus strength $\sigma\approx A$. Thus, enhancement of information transfer through the system due to serial correlation is best pronounced for weak stimuli. For both, extremely weak ($\sigma<A$) and for strong ($\sigma>A$) stimuli the information gain tends to vanish. The same observation was made in the previous work on negative serial correlations [24,29]. For vanishing stimuli information rates of both model vanish. On the other hand, strong stimuli $\sigma>A$ overwhelm epithelial oscillations, so that nonrenewal dynamics does not matter, hence mutual information rates of both models coincide.

The dependence of mutual information rates on the cutoff frequency of Gaussian stimuli [Fig. 4(b)] also showed nonmonotonous dependence. The stimulus variance was held constant when f_c was varied. Thus, an increase of cutoff frequency resulted in corresponding decrease of height of stimulus spectral density. In the limit of large cutoff frequencies the stimulus intensity vanishes and so must the response of the system. On the other hand, shrinking the stimulus band results in a decrease in the information available for the system. As a result, mutual information rates of both models decreased for low and high cutoff frequencies undergoing a maximum at 15–20 Hz, depending on the ratio of the afferent to epithelial oscillation frequencies w. The difference of information rates $\Delta\mathcal{I}$ repeated a bell-shaped curve of mutual information rate of the original model. The exact position of

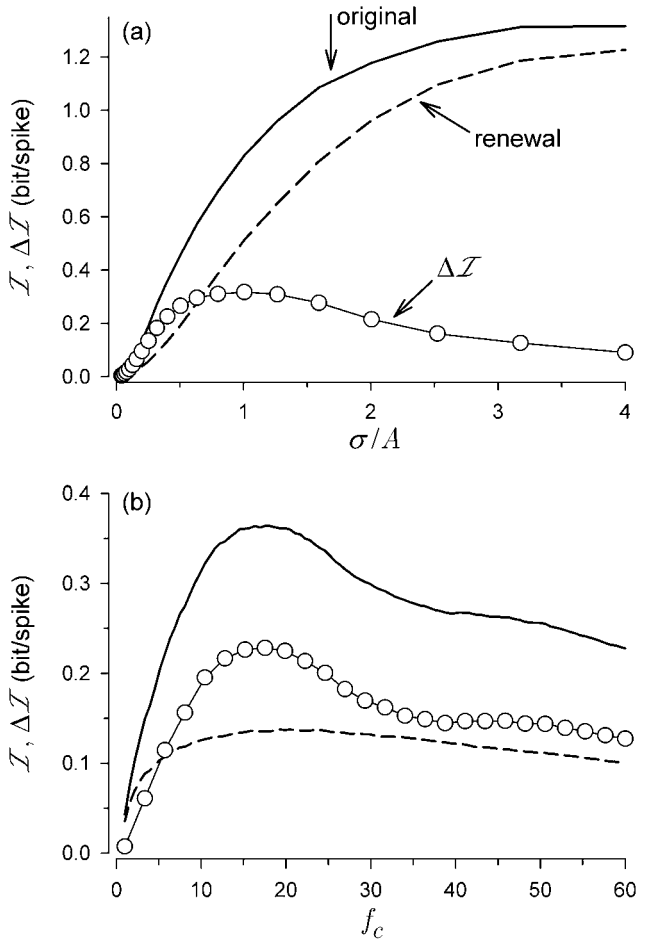

FIG. 4. Mutual information rates of the original (solid line), renewal (dashed line) models, and the information gain $\Delta\mathcal{I}$ (circles) versus stimulus parameters. (a) $\mathcal{I}$, $\Delta\mathcal{I}$ versus stimulus standard deviation normalized to the strength of epithelial oscillations σ/A for the fixed stimulus cutoff frequency f_c=20 Hz. (b) $\mathcal{I}$, $\Delta\mathcal{I}$ versus stimulus cutoff frequency for σ=0.2. Other parameters were the same as in Fig. 1.

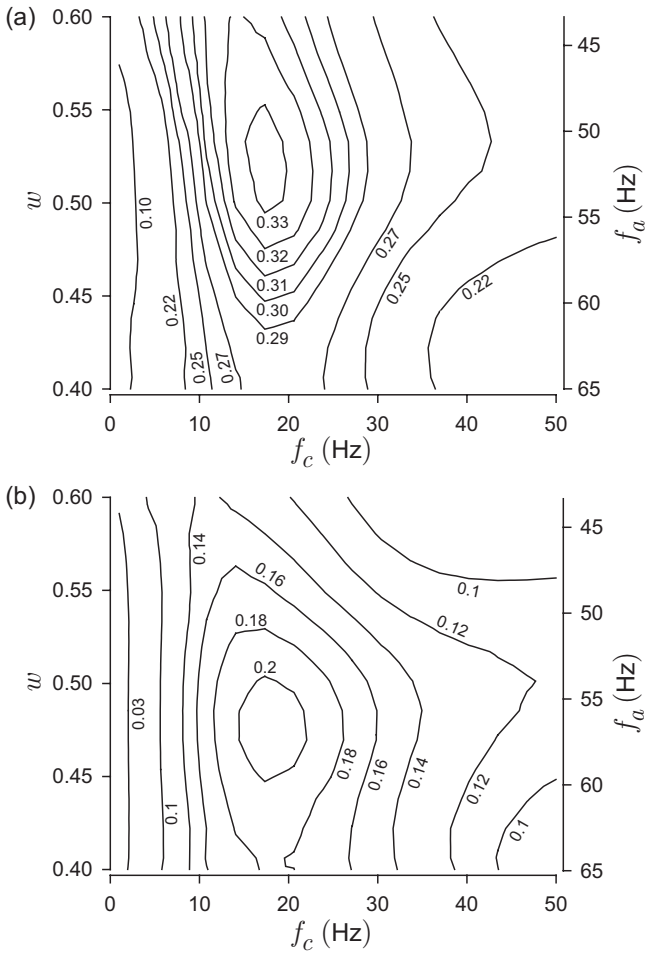

FIG. 5. Contour lines of the mutual information rate of the original model $\mathcal{I}$ (a) and the information gain $\Delta\mathcal{I}$ (b) versus the ratio of the epithelial to afferent oscillation frequencies $w=f_e/f_a$ and the stimulus cutoff frequency f_c. Corresponding frequency of AO, f_a, is given on the right vertical axes. The stimulus standard deviation was σ=0.2. Other parameters are the same as in Fig. 1.

the maximum is set by the relation of the stimulus cutoff frequency and peaks frequencies in the afferent power spectrum. The region of the low-frequency shaping due to serial correlations is limited by a critical point at which PSDs of the original and renewal models cross each other for the first time [24,29] [see Fig. 1(d)]. For $w \leqslant 0.5$ the first intersection of renewal spectrum occurs with the epithelial oscillation peak f_e, while for $w \geqslant 0.5$ the first intersection occurs with the sideband $f_a - f_e$. These peaks represent internal noise in the system. Depending on the stimulus cutoff frequency either peaks can appear to be within the stimulus band, worsening information transmission through the original system. Similar resonancelike dependence of mutual information rate vs stimulus cutoff frequency was reported in experimental study [19] for *P*-type electroreceptors and in theoretical works [24,29] for a model with short-term negative ISIs correlations. The dependence of mutual information rate on the frequency ratio w and on the stimulus cutoff frequency f_c for the fixed stimulus strength is summarized in Fig. 5.

Both, the mutual information rate of the original model and the information gain due to epithelial oscillations possess a global maximum. The location of the maximum of the mutual information rate occurs at w=0.53 and f_c=17 Hz. The maximum of the gain in mutual information occurs at the same cutoff frequency, but at w=0.47.

IV. CONCLUSION

We used a minimal model to study information transmission through a receptor system composed of two unidirectionally coupled stochastic oscillators. Such an organization was found in the peripheral electrosensory system of paddlefish [12] and is likely to be the case for other ampullary electroreceptors found in sharks and rays. In this system only one oscillator residing in sensory neuron is affected by the stimulus, while the other oscillator, residing in population of epithelial cells is invariant with respect to stimulation, acting as a source of internal narrow-band noise. In the model, the epithelial oscillations were mimicked by Gaussian narrow-band noise with the spectral peak at f_e=26 Hz and the width

1.4 Hz, as observed in experiments with paddlefish electroreceptors [12]. The afferent neuron was modeled by the canonical theta neuron system. The firing rate of the neuron was varied in the range 40–70 Hz. Epithelial oscillations modulate afferent firing leading to extended serial correlations of ISI. Because the ratio of the epithelial to afferent oscillation frequencies is in the range 0.4-0.6 the first lag of serial correlation coefficient is always negative [30] leading to enhanced order in the sequence of ISI, where a short interspike interval is followed by long interval, and vice versa [49]. Serial correlations extended to several dozens of ISI depending on the ratio of epithelial to afferent oscillation frequencies.

We have contrasted transmission of a Gaussian bandlimited signal through two model systems: (i) The original system with epithelial oscillations and hence nonrenewal spontaneous firing of afferent neuron and (ii) the renewal system with epithelial oscillations turned off and with parameters tuned to match the first order statistics of the original system. The coherence between the stimulus and spike trains was significantly (2-3 times) higher for the original model as compared to renewal model, indicating much better signal transmission through the model with epithelial oscillations. We have characterized this further by calculating the lower bound of mutual information rate, showing that the mutual information rate of the original model is significantly higher than that of corresponding renewal model. Thus, epithelial oscillations act to increase low-frequency signal transmission as we hypothesized before [12,30]. Furthermore, the mutual information rate and the gain in information rate due to epithelial oscillations showed nonmonotonous dependence on the ratio of the epithelial to afferent oscillation frequencies w being maximal at w close to 0.5, corresponding to longest ISI correlations. Similar to previous studies on negative serial correlations [19,24,29] we have found a nonmonotonous dependence of the mutual information rate on the stimulus parameters. The information about the stimulus encoded in the afferent spike train is maximized for a stimulus strength not exceeding the strength of epithelial oscillations, and for the stimulus cutoff frequencies in the range 17–20 Hz. The mutual information rate vanished at low stimulus cutoff frequencies. Low frequency stimuli in the range 0.1–1 Hz may be encountered by electroreceptors when an animal is slowly passing a dipolelike source of electric field [17]. For such low-frequency stimuli a signal detection theory is more appropriate than information measures used here [19]. Previous studies [19,24] have shown that negative ISI correlations suppress low-frequency noise power decreasing variability of neural responses to low-frequency stimuli and thus significantly enhance information transmission through the system. However, the origin of negative correlations in these studies was rooted in the internal properties of the sensory neuron itself, such as slow adaptation currents or threshold fatigue. As a result, the serial correlation coefficient showed just one significant negative value at the first lag. The mechanism of serial correlations in our model is different, since the epithelial oscillation were the main source of long-lasting oscillatory serial correlations [30].

Although the parameters of our model were tuned to match spontaneous and response properties of eletroreceptors in paddlefish, our results are applicable to general situations of spiking neurons perturbed by colored noise. Previous work considered influence of exponentially correlated noise [20,50,51], resulting in positive exponential serial correlations. Here we studied the case of narrow-band noise and showed that such internal noise results in significant improvement of low-frequency signal transmission through the system.

ACKNOWLEDGMENTS

The authors thank D.F. Russell and L. Schimansky-Geier for valuable discussions. This work was supported by National Institutes of Health Grant No. DC04922 and by the Biomimetic Nanoscience and Nanotechnology program of Ohio University. I.F. was supported by the Schlumberger Foundation.

[1] S. Camalet, T. Duke, F. Julicher, and J. Prost, Proc. Natl. Acad. Sci. U.S.A. **97**, 3183 (2000).
[2] P. Martin, D. Bozovic, Y. Choe, and A. J. Hudspeth, J. Neurosci. **23**, 4533 (2003).
[3] P. Martin and A. J. Hudspeth, Proc. Natl. Acad. Sci. U.S.A. **96**, 14306 (1999).
[4] L. Catacuzzeno, B. Fioretti, P. Perin, and F. Franciolini, J. Physiol. (London) **561**, 685 (2004).
[5] F. Jorgensen and A. B. Kroese, Acta Physiol. Scand. **185**, 271 (2005).
[6] S. G. Sadeghi, M. J. Chacron, M. C. Taylor, and K. E. Cullen, J. Neurosci. **27**, 771 (2007).
[7] V. M. Eguiluz, M. Ospeck, Y. Choe, A. J. Hudspeth, and M. O. Magnasco, Phys. Rev. Lett. **84**, 5232 (2000).
[8] W. T. Clusin and M. V. Bennett, J. Gen. Physiol. **73**, 703 (1979).
[9] W. Clusin and M. Bennett, J. Gen. Physiol. **73**, 685 (1979).
[10] J. Lu and H. M. Fishman, Biophys. J. **69**, 2458 (1995).
[11] A. Neiman and D. F. Russell, Phys. Rev. Lett. **86**, 3443 (2001).
[12] A. B. Neiman and D. F. Russell, J. Neurophysiol. **92**, 492 (2004).
[13] D. F. Russell, L. A. Wilkens, and F. Moss, Nature (London) **402**, 291 (1999).
[14] L. Wilkens, D. Russell, X. Pei, and C. Gurgens, Proc. R. Soc. London, Ser. B **264**, 1723 (1997).
[15] L. A. Wilkens, B. Wettring, E. Wagner, W. Wojtenek, and D. F. Russell, J. Exp. Biol. **204**, 1381 (2001).
[16] M. H. Hofmann, B. Chagnaud, and L. A. Wilkens, J. Exp. Biol. **208**, 4213 (2005).
[17] M. H. Hofmann and L. A. Wilkens, Phys. Biol. **2**, 23 (2005).
[18] R. Ratnam and M. E. Nelson, J. Neurosci. **20**, 6672 (2000).
[19] M. J. Chacron, A. Longtin, and L. Maler, J. Neurosci. **21**, 5328 (2001).

[20] B. Lindner, Phys. Rev. E **69**, 022901 (2004).
[21] E. Müller, L. Buesing, J. Schemmel, and K. Meier, Neural Comput. **19**, 2958 (2007).
[22] M. P. Nawrot, C. Boucsein, V. Rodriguez-Molina, A. Aertsen, S. Grun, and S. Rotter, Neurocomputing **70**, 1717 (2007).
[23] M. Chacron, L. Maler, and J. Bastian, Nat. Neurosci. **8**, 673 (2005).
[24] M. J. Chacron, B. Lindner, and A. Longtin, Phys. Rev. Lett. **92**, 080601 (2004).
[25] X. J. Wang, J. Neurophysiol. **79**, 1549 (1998).
[26] Y. H. Liu and X. J. Wang, J. Comput. Neurosci. **10**, 25 (2001).
[27] J. Benda, A. Longtin, and L. Maler, J. Neurosci. **25**, 2312 (2005).
[28] M. J. Chacron, B. Lindner, and A. Longtin, J. Comput. Neurosci. **23**, 301 (2007).
[29] B. Lindner, M. J. Chacron, and A. Longtin, Phys. Rev. E **72**, 021911 (2005).
[30] A. B. Neiman and D. F. Russell, Phys. Rev. E **71**, 061915 (2005).
[31] G. B. Ermentrout and N. Kopell, SIAM J. Appl. Math. **46**, 233 (1986).
[32] B. Ermentrout, Neural Comput. **10**, 1721 (1998).
[33] E. M. Izhikevich, *Dynamical Systems in Neuroscience the Geometry of Excitability and Bursting* (MIT Press, Cambridge, MA, 2007).
[34] B. S. Gutkin and G. B. Ermentrout, Neural Comput. **10**, 1047 (1998).
[35] B. Lindner, A. Longtin, and A. Bulsara, Neural Comput. **15**, 1760 (2003).
[36] C. Borgers and N. Kopell, Neural Comput. **17**, 557 (2005).
[37] C. Borgers and N. Kopell, Neural Comput. **15**, 509 (2003).
[38] L. Schimansky-Geier and C. Zülicke, Z. Phys. B **79**, 451 (1990).
[39] C. W. Gardiner, *Handbook of Stochastic Methods for Physics, Chemistry, and the Natural Sciences*, 3rd ed (Springer, Berlin, 2004).
[40] F. Gabbiani and C. Koch, in *Computational Neuroscience*, edited by C. Koch and I. Segev. 2nd ed. (MIT Press, Cambridge, MA, 1998), pp. 313–360.
[41] J. S. Bendat and A. G. Piersol, *Random Data Analyis and Measurement Procedures*, 3rd ed (Wiley, New York, 2000).
[42] W. Bialek, F. Rieke, R. R. de Ruyter van Steveninck, and D. Warland, Science **252**, 1854 (1991).
[43] F. Gabbiani and W. Metzner, J. Exp. Biol. **202**, 1267 (1999).
[44] A. Borst and F. E. Theunissen, Nat. Neurosci. **2**, 947 (1999).
[45] D. R. Cox, *The Statistical Analysis of Series of Events* (Wiley, New York, 1966).
[46] S. Kullback and R. A. Leibler, Ann. Math. Stat. **22**, 79 (1951).
[47] S. Liepelt, J. A. Freund, L. Schimansky-Geier, A. Neiman, and D. F. Russell, J. Theor. Biol. **237**, 30 (2005).
[48] A. Neiman, L. Schimansky-Geier, and F. Moss, Phys. Rev. E **56**, R9 (1997).
[49] M. J. Chacron, A. Longtin, M. St-Hilaire, and L. Maler, Phys. Rev. Lett. **85**, 1576 (2000).
[50] J. W. Middleton, M. J. Chacron, B. Lindner, and A. Longtin, Phys. Rev. E **68**, 021920 (2003).
[51] T. Schwalger and L. Schimansky-Geier, Phys. Rev. E **77**, 031914 (2008).